Amplitude analysis of $\eta\pi$ final states at glueX

C. Gleason (For the GlueX Collaboration)

Union College, 807 Union Street Schenectady, NY 12308.

The primary goal of the GlueX experiment at Jefferson Lab is to map the spectrum of light hybrid mesons. GlueX, which has a linearly polarized photon beam and a large acceptance for both charged and neutral particles, has access to both the neutral, $\gamma p \to \eta\pi^0 p$, and charged, $\gamma p \to \eta\pi^- \Delta^{++}$, final states. These proceedings will discuss the amplitude analysis of $\eta\pi$ channels at GlueX with a focus on the study of the production of the $a_2(1320)$ meson as function of Mandelstam t.

1. Introduction

GlueX is a photoproduction experiment located in Hall-D at the Thomas Jefferson National Accelerator Facility in Newport News, VA, which aims to study how hadrons are generated from Quantum Chromodynamics (QCD). The main goal of GlueX is to map the spectrum of light-quark hybrid mesons, for which a broad spectrum has been predicted in Lattice QCD calculations [1]. Many experiments have searched for hybrids in their decays to $\eta\pi$ and $\eta'\pi$ final-states [2-14]. One of the main benefits of studying the $\eta^{(')}\pi$ systems is that exotic quantum numbers (J^{PC}) naturally emerge if the system is observed in an odd orbital angular momentum state. These exotic quantum numbers can not be created from a traditional meson ($q\bar{q}$) state. Recently, the Joint Physics Analysis Center (JPAC) Collaboration determined the resonance pole parameters for the lightest hybrid, the $\pi_1(1600)$, by performing a coupled channel analysis on COMPASS data for $\eta\pi$ and $\eta'\pi$ [15]. GlueX will seek to confirm the pole position of the $\pi_1(1600)$ and determine its production mechanism.

The GlueX experiment is summarized elsewhere and in these proceedings [16,17]. We are building the foundation for hybrid searches by studying the photoproduction of $a_{0,2} \to \eta\pi$, with a focus on studying $a_2(1320)$ production as a function of momentum transfer, $-t$. It is expected that the a_2^- and π_1^- will be produced via π exchange, while the neutral a_2^0 and π_1^0 will be produced via natural (ρ, ω) exchanges. Therefore, understanding the production mechanism of the well-known a_2 will be crucial to identifying hybrids decaying into $\eta^{(')}\pi$ final states. Due to its large acceptance for neutral and charged final state particles, GlueX can access the charged, $a_2^- \to \eta\pi^-$, and neutral, $a_2^0 \to \eta\pi^0$, final states. The charged and neutral decay modes are complementary to each other and are expected to have different production mechanisms that can be determined by using GlueX's linearly polarized photon beam. Additionally, GlueX can measure different decay modes of the η, such as $\eta \to \gamma\gamma$ and $\eta \to \pi^+\pi^-\pi^0$.

These decay modes should contain the same physics, but can have different acceptances and backgrounds. Showing that we can robustly extract the a_2 signal for the different decay modes is important to show that the acceptance of GlueX is well understood.

The angular distribution of the $\eta\pi$ system can be described in the Gottfried-Jackson (GJ) frame. In the GJ frame, the meson (*e.g.* the a_2) is at rest, the z-axis is defined along the photon beam's momentum in the center-of-mass frame, and the y axis is perpendicular to the production plane. The angle θ_{GJ} is the decay angle of the η with respect to the z-axis. Figures 1a) and 1b) show $\cos\theta_{GJ}$ as a function of $\eta\pi$ mass for the neutral (a) and charged (b) decay modes for $0.1 < -t < 0.3$ GeV^2 (not corrected for acceptance). The main features seen in the distributions are enhancements for the $a_0(980)$ and $a_2(1320)$. One interesting feature we can see is that the $\cos\theta_{GJ}$ distribution of the a_2 differs between the charged and neutral channels. While this could be caused by a difference in acceptance between the charged and neutral channels, these plots suggest that the neutral and charged a_2's intensity have different D-wave spin projection (m) contributions.

2. Results

GlueX has measured beam asymmetries to determine the production mechanisms of single pseudoscalar production and is in the process of extracting Spin Density Matrix Elements (SDMEs) for vector meson production [17-21]. The next step is to study the production mechanism of well established mesons, such as the $a_{0,2}$, that decay into $\eta\pi$ final states. It is expected from Lattice QCD that the $\pi_1(1600)$ decay to $\eta\pi$ final states is suppressed with respect to other channels [22]. Studying the production of the $a_{0,2} \to \eta\pi$ allows us to develop the tools and techniques needed to study other two pseudoscalar final states, such as $\eta'\pi$ where there is expected to be a much larger $\pi_1(1600)$ signal [22].
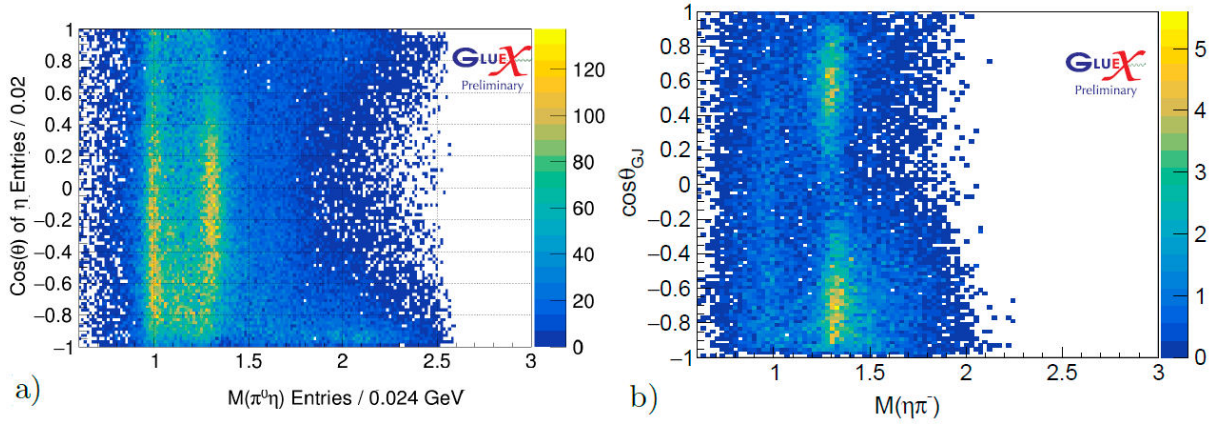
FIGURE 1. $\cos\theta_{GJ}$ as a function of $M(\eta\pi^0)$ a) and $M(\eta\pi^-)$ b) for $0.1 < -t < 0.3$ GeV^2.
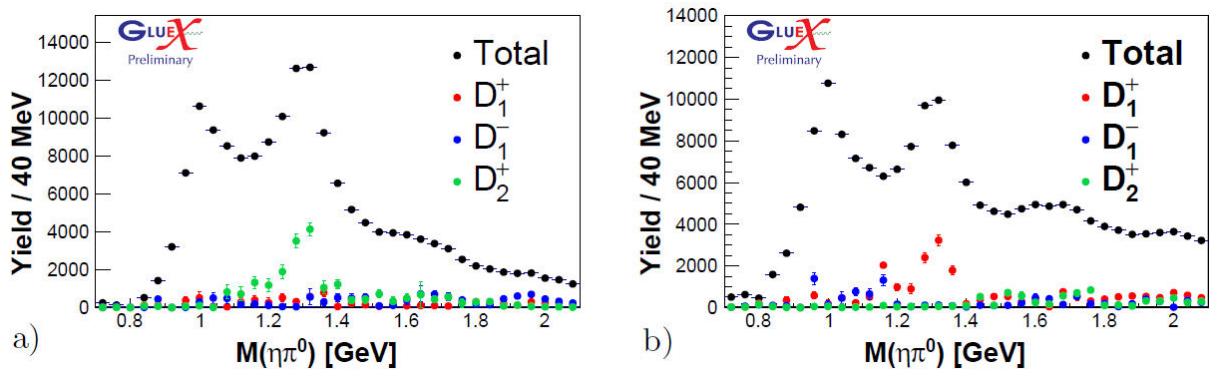
FIGURE 2. Preliminary results of an amplitude analysis of $\eta\pi^0$ for $0.1 < -t < 0.3$ GeV^2 a) and $0.3 < -t < 0.6$ GeV^2 b).

JPAC has derived polarized amplitudes for two pseudoscalar production [23]. The polarized intensity is given by,

$$I(\Omega, \Phi) = 2\kappa \sum_k \left\{ (1 - P_\gamma) \left| \sum_{\ell,m} [[\ell]^-_{m,k} \text{Re}[Z^m_\ell(\Omega, \Phi)] \right|^2 + (1 - P_\gamma) \left| \sum_{\ell,m} [[\ell]^+_{m,k} \text{Im}[Z^m_\ell(\Omega, \Phi)] \right|^2 \right.$$

$$\left. + (1 + P_\gamma) \left| \sum_{\ell,m} [[\ell]^+_{m,k} \text{Re}[Z^m_\ell(\Omega, \Phi)] \right|^2 + (1 + P_\gamma) \left| \sum_{\ell,m} [[\ell]^-_{m,k} \text{Im}[Z^m_\ell(\Omega, \Phi)] \right|^2 \right\}. \tag{1}$$

The basis is $Z^m_\ell(\Omega, \Phi) = Y^m_\ell(\Omega)e^{-i\Phi}$, where Φ is the polarization angle of the photon beam with respect to the production plane, Ω are the decay angles of the η in the $\eta\pi$ helicity frame, Y^m_ℓ are the spherical harmonics, and ℓ, m are the spin quantum number and its projection, respectively. The coefficients $[\ell]^\epsilon_{m;k}$ are fit to the data to extract the amplitudes for the corresponding partial waves. The reflectivity, $\epsilon = \pm$, corresponds to the naturality, $\eta = P(-1)^J$, of the exchange particle at leading order in the total energy. The starting wave set ($S^\pm_0$, $D^+_{0,1,2}$, $D^-_{-1,0,1}$) was chosen from a tensor meson decay model from JPAC [24]. The tensor meson decay model from JPAC accurately describes the a^0_2 cross-section measurements from CLAS, predicts a^0_2 production to be dominated by natural exchanges, and provides us with a minimal starting wave set [24,25]. While this model does not make any predictions for the charged channel, the same wave set was chosen for consistency.

2.1. $\gamma p \rightarrow \eta\pi^0 p$

Figures 2a) and 2b) show the preliminary fit results for select partial waves in two $-t$ bins: $0.1 < -t < 0.3$ GeV^2 (a) and $0.3 < -t < 0.6$ GeV^2 (b). The black points represent the total intensity, the red points represent the D^+_1 intensity, the blue points represent the D^-_1 intensity, and the green points represent the D^+_2 intensity. The D^+_2 has the largest intensity for $0.1 < -t < 0.3$ GeV^2 and the D^+_1 has the largest intensity for $0.3 < -t < 0.6$. This suggests that natural exchange (ρ, ω) is the dominant production mechanism for these two $-t$ bins. This agrees with the GlueX results for the beam asymmetries in the production of η and π^0 [20,21].
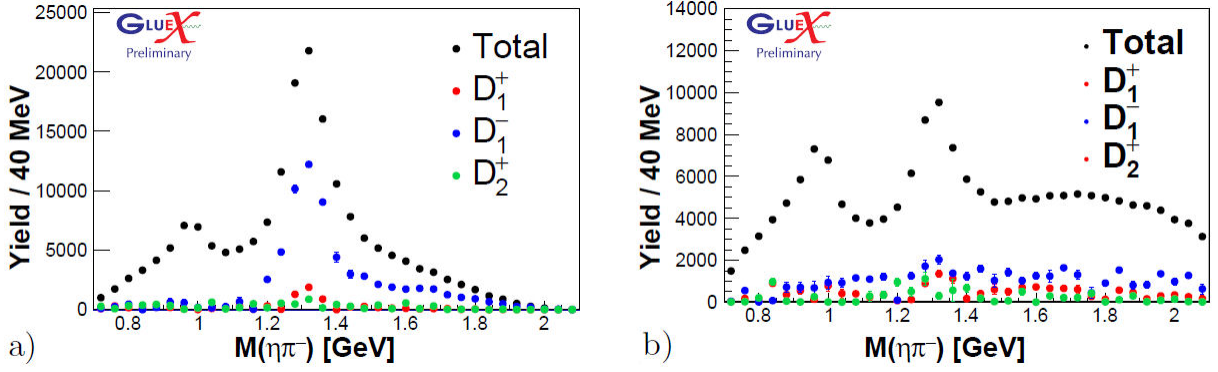
FIGURE 3. Preliminary results of an amplitude analysis of $\eta\pi^-$ for $0.1 < -t < 0.3$ GeV^2 a) and $0.3 < -t < 0.6$ GeV^2 b).
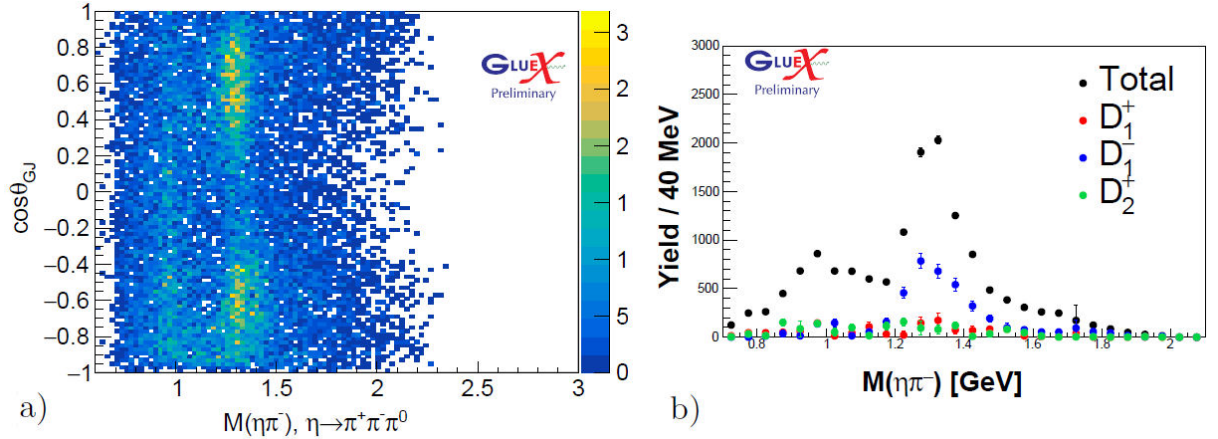
FIGURE 4. a) $\cos\theta_{GJ}$ as a function of $M(\eta\pi^-)$ for $\eta \to \pi^+\pi^-\pi^0$. b) Preliminary results of an amplitude analysis of $\eta\pi^-$, $\eta \to \pi^+\pi^-\pi^0$ for $0.1 < -t < 0.3$ GeV^2.

2.2. $\gamma p \to \eta\pi^- \Delta^{++}$

Figures 3a) and 3b) show the preliminary fit results for select partial waves in the charged channel. The dominant partial wave for $0.1 < -t < 0.3$ GeV^2 is the D_1^-, suggesting that the dominant production mechanism is unnatural (π) exchange. For $0.3 < -t < 0.6$ GeV^2, the D_1^- and D_1^+ partial waves are comparable in the region of the $a_2(1320)$. The D_0^+ wave, which is not drawn here, also contributes about the same amount as these two partial waves. This result suggests that natural (ρ) and unnatural (π) parity exchanges are equivalent in this $-t$ region. These conclusions agree with what was seen in the π^- beam asymmetries, which show that unnatural parity exchange dominates at these photon beam energies and small values of $-t$ [18]. As $-t$ increases, the beam asymmetry transitions from unnatural to natural parity exchange dominance around $-t = 0.5$ GeV^2.

An amplitude analysis was also performed on the $\eta \to \pi^+\pi^-\pi^0$ decay mode as a cross-check. The different decay modes of the η should contain the same information about a_2^- decay, but they have different acceptances and backgrounds. Figure 4a) shows the $\cos\theta_{GJ}$ distribution as a function of $\eta\pi^-$ mass for $0.1 < -t < 0.3$ GeV^2. Similar features are seen when comparing the $\gamma\gamma$ decay (Fig. 1b)) and $\pi^+\pi^-\pi^0$ de-

cay. Figure 4b shows the preliminary results of the amplitude analysis for $0.1 < -t < 0.3$ GeV^2. Like the $\gamma\gamma$ decay mode, the dominating feature in the $\pi^+\pi^-\pi^0$ decay mode is the D_1^- wave (blue points). As a first step, this agreement shows that the acceptance of the GlueX spectrometer is being treated correctly.

3. Summary

GlueX is building the foundation for hybrid meson searches by studying the decays of $a_{0,2} \to \eta\pi$. Establishing the production mechanism as a function of $-t$ will be crucial to identifying the $\pi_1(1600) \to \eta^{(')}\pi$. These proceedings presented preliminary results of an amplitude analysis on $\eta\pi^0$ and $\eta\pi^-$ for two different $-t$ bins. For the first time, we have used polarized amplitudes to determine the dominant partial waves and production mechanisms. At low $-t$, we see that natural exchanges (ρ, ω) dominate for a_2^0 production and unnatural (π) for a_2^- production. As $-t$ increases, natural exchanges continue to dominate for a_2^0, while the natural and unnatural exchanges are comparable for the a_2^-. Additionally, we also observe that the D-wave spin projection (m) for the a_2 depends on $-t$. This work is part of a larger program at GlueX to develop the amplitude analysis tools needed in hybrid me-

son searches, and is a necessary first step to extracting the small $\pi_1(1600)$ contribution. These tools can be applied to other two pseudoscalar final states, such as $\eta'\pi$.

---

1. J. J. Dudek *et al.* Toward the excited isoscalar meson spectrum from lattice QCD. *Phys. Rev. D* **88.9** (2013) 094505. https://doi.org/10.1103/PhysRevD.88.094505.

2. D. Alde *et al.* Evidence for a 1^{+-} Exotic Meson. *Phys. Lett. B* **205** (1988) 397. https://doi.org/10.1016/0370-2693(88)91686-3.

3. H. Aoyagi *et al.*, Study of the $\eta\pi^-$ system in the π^-p reaction at 6.3 GeV/c. *Phys. Lett. B* **314** (1993) 246-254. https://doi.org/10.1016/0370-2693(93)90456-R.

4. G. M. Beladidze *et al.*, Study of π^-pN$\rightarrow$ $\eta\pi^-p$ and $\pi N \rightarrow \eta'\pi - N$ reactions at 37 GeV/c. *Phys. Lett. B* **313** (1993) 276, https://doi.org/10.1016/0370-2693(93)91224-B.

5. Yu. P. Gouz *et al.*, Study of the wave with $JPC = 1^{-+}$ in the partial wave analysis of $\eta'\pi^-$, $\eta\pi^- f_1\pi^-$ and $\rho^0\pi^-$ systems produced in π^-N interactions at $P_{\pi^-} = 37$ GeV/c. *AIP Conf. Proc.* **272** (2008) 572-576. https://doi.org/10.1063/1.43520.

6. D. V. Amelin *et al.* Investigation of hybrid states in the VES experiment at the Institute for High Energy Physics (Protvino). *Phys. Atom. Nucl.* **68** (2005) 359-371. https://doi.org/10.1134/1.1891185.

7. V. Dorofeev, New results from VES. *Frascati Phys. Ser.* **15** (1999) 3.

8. D. R. Thompson *et al.* Evidence for exotic meson production in the reaction $\pi^-p \rightarrow \eta\pi^-$ at 18 GeV/c. *Phys. Rev. Lett.* **79** (1997) 1630. https://doi.org/10.1103/PhysRevLett.79.1630.

9. G. S. Adams *et al.*, Confirmation of a π_1^0 Exotic Meson in the $\eta\pi^0$ System. *Phys. Lett. B* **657** (2007) 27, https://doi.org/10.1016/j.physletb.2007.07.068.

10. E. I. Ivanov *et al.*, Observation of exotic meson production in the reaction $\pi^- \rightarrow \eta'\pi p$ at 18 GeV/c. *Phys. Rev. Lett.* **86** (2001) 3977. https://doi.1103/PhysRevLett.86.3977.

11. A. Abele *et al.*, Exotic $\pi\eta$ state in anti-p d annihilation at rest into $\pi^0\pi^+\pi^-$(spectator). *Phys. Lett. B* **423** (1998) 175. https://doi.org/10.1016/S0370-2693(98)00123-3.

12. A. Abele *et al.*, Evidence for a $\pi\eta$ P wave in anti-p p annihilations at rest into $\pi^0\pi^0\eta$. *Phys. Lett. B* **446** (1999) 349, https://doi.org/10.1016/S0370-2693(98)01544-5.

13. G. S. Adams *et al.*, Amplitude analyses of the decays $\chi_{c1} \rightarrow \eta\pi^+\pi^-$ and $\chi_{c1} \rightarrow \eta'\pi^+\pi^-$. *Phys. Rev. D* **84** (2011) 112009. https://doi.org/10.1103/PhysRevD.84.112009.

14. C. Adolph *et al.* Odd and even partial waves of $\eta\pi^-$ and $\eta'\pi^-$ in $\pi^-p \rightarrow \eta'\pi^-p$ at 191 GeV/c. *Phys. Let. B* **740** (2015) 303. issn: 0370-2693. https://doi.org/10.1016/j.physletb.2014.11.058.

15. A. Rodas *et al.* Determination of the pole position of the lightest hybrid meson candidate. *Phys. Rev. Lett.* **122.4** (2019) 042002. https://doi.org/10.1103/PhysRevLett.122.042002.

16. S. Adhikari *et al.*, The GlueX beamline and detector. *Nuclear Instruments and Methods in Physics Research Section A: Accelerators, Spectrometers, Detectors and Associated Equipment* **987** (2021) 164807, https://doi.org/10.1016/j.nima.2020.164807.

17. P. Pauli, Accessing glue through photoproduction measurements at GlueX. In: 19th International Conference on Hadron Spectroscopy and Structure. Dec. 2021. arXiv:2112.05633[hep-ex].

18. S. Adhikari *et al.*, Measurement of beam asymmetry for $\pi^-\Delta^{++}$ photoproduction on the proton at $E_\gamma = 8.5$ GeV. *Phys. Rev. C* **103** (2021) L022201. https://doi.org/10.1103/PhysRevC.103.L022201.

19. S. Adhikari *et al.* Measurement of the photon beam asymmetry in $\gamma \rightarrow K^+ \sum^0$ at $E'_\gamma = 8.5$ GeV . In: Phys. Rev. C 101 (6 June 2020), p. 065206. https://doi.org/10.1103/PhysRevC.101.065206.

20. S. Adhikari *et al.* Beam asymmetry $\sum$ for the photoproduction of η and η' mesons at $E_\gamma = 8.8$ GeV. *Phys. Rev. C* **100** (2019) 052201. https://doi.org/10.1103/PhysRevC.100.052201.

21. H. Al Ghoul *et al.* Measurement of the beam asymmetry $\sum$ for π^0 and η photoproduction on the proton at $E_\gamma = 9$ GeV. *Phys. Rev. C* **95** (2017) 042201. https://doi.org/10.1103/PhysRevC.95.042201.

22. A. J. Woss *et al.* Decays of an exotic 1-+ hybrid meson resonance in QCD. *Phys. Rev. D* **103.5** (2021) 054502. https://doi.org/10.1103/PhysRevD.103.054502.

23. V. Mathieu *et al.* Moments of angular distribution and beam asymmetries in $\eta\pi^0$ photoproduction at GlueX. *Phys. Rev. D* **100** (2019) 054017, https://doi.org/10.1103/PhysRevD.100.054017.

24. V. Mathieu *et al.*, Exclusive tensor meson photoproduction. *Phys. Rev. D* **102** (2020) 014003. https://doi.org/10.1103/PhysRevD.102.014003.

25. A. Celentano *et al.* First measurement of direct photoproduction of the $a_2(1320)^0$ meson on the proton. *Phys. Rev. C* **102** (2020) 032201. https://doi.org/10.1103/PhysRevC.102.032201.